

## Spin-Orbit Coupling-Induced Magnetic Phase in the $d$ -Density-Wave Phase of $\text{La}_{2-x}\text{Ba}_x\text{CuO}_4$ Superconductors

Congjun Wu,<sup>1,2</sup> Jan Zaanen,<sup>1,\*</sup> and Shou-Cheng Zhang<sup>1</sup>

<sup>1</sup>*Department of Physics, McCullough Building, Stanford University, Stanford, California 94305-4045, USA*

<sup>2</sup>*Kavli Institute for Theoretical Physics, University of California, Santa Barbara, California 93106, USA*

(Received 22 May 2005; published 8 December 2005)

We study the effects of spin-orbit coupling in the  $d$ -density wave (DDW) phase. In the low-temperature orthorhombic phase of  $\text{La}_{2-x}\text{Ba}_x\text{CuO}_4$ , we find that spin-orbit coupling induces ferromagnetic moments in the DDW phase, which are polarized along the [110] direction with a considerable magnitude. This effect does not exist in the superconducting phase. On the other hand, if the  $d$ -density wave order does not exist at zero field, a magnetic field along the [110] direction always induces such a staggered orbital current. We discuss experimental constraints on the DDW states in light of our theoretical predictions.

DOI: 10.1103/PhysRevLett.95.247007

PACS numbers: 74.25.Ha, 74.20.Mn, 74.20.Rp, 74.25.Bt

The mechanism of the pseudogap phenomena in high  $T_c$  superconductors remains controversial. Chakravarty *et al.* [1] proposed that it may originate from a hidden long-range  $d$ -density wave (DDW) order [2,3], which competes with the  $d$ -wave superconductivity (DSC). This scenario has aroused much interest. Extensive analytic and numerical investigations have shown its existence under certain conditions in a variety of one- and two-dimensional systems [4–8]. However, these states are hard to detect experimentally and results are still controversial [9]. Polarized neutron scattering experiments [10,11] in  $\text{YBa}_2\text{CuO}_{6+x}$  show some supporting evidence. On the other hand, Stock *et al.* [12] found no indication of this phase using nonpolarized neutron beams.

Recently, spin-orbit (SO) coupling has received much attention in the emerging science of spintronics. Murakami, Nagaosa, and Zhang proposed the intrinsic spin-Hall effect through SO coupling in the  $p$ -doped semiconductors to generate the dissipationless spin current using electrical fields [13]. Similar effects were also predicted in the  $n$ -doped systems [14]. The spin-Hall effect in GaAs has already been observed experimentally [15].

In Mott insulators, SO coupling also has important effects on the Heisenberg superexchange interactions, which is responsible for the anisotropic correction termed the Dzyaloshinskii-Moriya (DM) interaction [16]. Given the intrinsic spin-Hall effect in the semiconductors, it is natural to ask what happens in the presence of SO coupling with states carrying spontaneous electrical currents like the DDW state. The answer turns out to depend on details, but these conspire in the  $\text{La}_2\text{CuO}_4$  system to give rise to an experimentally observable effect: as in the half-filled antiferromagnets, SO coupling gives rise to a weak planar ferromagnetism which can be used to detect this otherwise elusive phenomenon.

At zero temperature,  $\text{La}_{2-x}\text{Ba}_x\text{CuO}_4$  undergoes a structural phase transition from the low-temperature orthorhombic (LTO) phase to the low-temperature tetragonal (LTT) phase at doping  $\delta_c \approx 0.12$ . In the LTO phase of the un-

doped  $\text{La}_2\text{CuO}_4$ , the DM interaction originates from the staggered distortion pattern of the oxygen octahedra. It results in the antiferromagnetic moments lying in the  $ab$  plane and the weak ferromagnetic moments along the  $c$  axis [17]. By analogy, the DDW state exhibits staggered orbital moments. Without SO coupling, the DDW state decouples from the spin channel, which remains paramagnetic. However, SO coupling couples these two channels together, and thus orbital currents should affect spin and lead to observable effects.

In this Letter, we find that the staggered orbital current induces uniform ferromagnetic moments in both LTO and LTT phases. The moments lie in the [110] direction in the LTO phase and the [100] direction in the LTT phase, respectively. The magnitude per Cu site is at the order of several percent of one Bohr magneton, thus is detectable. Conversely, if the DDW order does not exist in the ground state, it can be induced by magnetic fields, suggesting that the degree of proximity to the instability can be in principle investigated as well.

We consider the mean field DDW Hamiltonian with SO coupling in the LTO phase:

$$\begin{aligned}
 H_{\text{MF}} = & \sum_{\langle ij \rangle \alpha \beta} \{ c_{i\alpha}^\dagger (-t_{\text{eff}} + i\vec{\lambda}_{ij} \cdot \vec{\sigma}_{\alpha\beta}) c_{j\beta} + \text{H.c.} \} \\
 & + i \sum_{\langle ij \rangle \sigma} \text{Im} \chi_{ij} (c_{i\alpha}^\dagger c_{j\alpha} - \text{H.c.}) - \mu \sum_{i\sigma} c_{i\sigma}^\dagger c_{i\sigma} \\
 & + \frac{1}{2V} \sum_{\langle ij \rangle} \text{Im} \chi_{ij} \text{Im} \chi_{ij}, \quad (1)
 \end{aligned}$$

where  $\langle ij \rangle$  indicates summation over the nearest neighbors only.  $\chi_{ij}$  is the decoupling of the Heisenberg exchange term in the particle-hole channel [3] as  $\chi_{ij} = V \langle c_{i\sigma}^\dagger c_{j\sigma} \rangle$ . Its imaginary part  $\text{Im} \chi_{ij}$  is the DDW order parameter and is treated self-consistently below. On the other hand,  $\text{Re} \chi_{ij}$  changes slowly within the parameter regime discussed below, thus is absorbed into the effective hopping integral  $t_{\text{eff}}$  which gives the bandwidth of holes. We choose

$t_{\text{eff}} \approx 100$  meV which is rescaled to 1 below. The SO coupling term  $\vec{\lambda}_{ij}$  is determined by the lattice symmetries [18] as shown in Fig. 1(a), such as (i) twofold rotations around the  $c$  axes passing the in-plane O sites, (ii) inversion symmetry with respect to Cu sites, and (iii) reflection symmetry with respect to the  $[110]$  direction. Consequently, it shows a staggered pattern  $\vec{\lambda}_{i,i+\hat{x}} = (-)^{i_x+i_y}(\lambda_1, \lambda_2, 0)$ ,  $\vec{\lambda}_{i,i+\hat{y}} = (-)^{i_x+i_y}(-\lambda_2, -\lambda_1, 0)$  [19].  $\vec{\lambda}_{ij}$  is almost perpendicular to the bond direction in the LTO phase [20], i.e.,  $\lambda_1 \ll \lambda_2$ , and  $\lambda_2$  is estimated to be around 2 meV [18]. In the LTO phase, the symmetries (ii) and (iii) still ensure the  $\text{Im}\chi_{ij}$  to exhibit the  $d_{x^2-y^2}$  pattern.

We first present physical arguments for the appearance of the ferromagnetic moments for a simplified case of  $\lambda_1 = \lambda_2 = \lambda/\sqrt{2}$ , and then show that the realistic values of  $\lambda_{1,2}$  essentially give the same result. In the simplified case, the SO coupling term plays the role of the staggered spin flux with the quantization axis along the  $[110]$  direction [19]. The effective Hamiltonian reads

$$H = \sum_k c_{k\alpha}^\dagger c_{k\alpha} (\epsilon_k - \mu) + 2if(\vec{k})c_{k\alpha}^\dagger \{ \lambda \sigma_{1,\alpha\beta} + \text{Im}\chi \delta_{\alpha\beta} \} c_{k+\vec{Q},\beta}, \quad (2)$$

where  $f(\vec{k}) = \cos k_x - \cos k_y$ ,  $\sigma_1 = (\sigma_x + \sigma_y)/\sqrt{2}$ ,  $\vec{Q} = (\pi, \pi)$ , and the spin index  $\alpha = \uparrow (\downarrow)$  refers to parallel (antiparallel) to the  $[110]$  direction. For  $\vec{k}$  around the nodes  $(\pm\pi/2, \pm\pi/2)$ , we define  $\vec{k}_{\parallel}$  and  $\vec{k}_{\perp}$  to be the projections of its deviation from the nodes on the directions parallel and perpendicular to the nested Fermi surface, respectively. As shown in Fig. 1(b), we obtain the anisotropic Dirac-cone-like dispersion relation with different slopes for spin  $\uparrow (\downarrow)$  electrons

$$E(k)_{a,\alpha} = \pm \sqrt{v_f^2 k_{\perp}^2 + 8(\text{Im}\chi \pm \lambda)^2 k_{\parallel}^2}, \quad (3)$$

where the first  $\pm$  on the right-hand side of Eq. (3) corre-

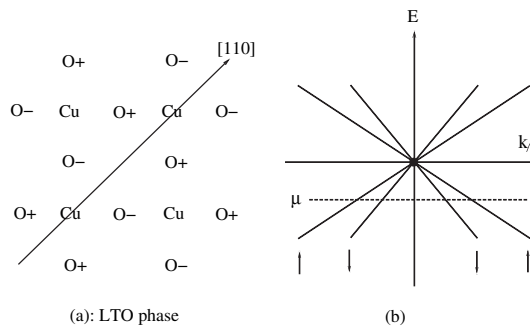


FIG. 1. (a) The lattice symmetry in the LTO phase.  $O^+$  ( $O^-$ ) denotes the oxygen atom moving into (out of) the  $\text{CuO}$  plane. The arrow indicates the  $[110]$  direction. (b) The anisotropic Dirac-cone-like dispersion relations around nodes  $(\pm\pi/2, \pm\pi/2)$  for spin parallel ( $\uparrow$ ) and antiparallel ( $\downarrow$ ) to the  $[110]$  direction.

sponds to the upper (lower) Dirac cone as denoted by the band index  $a$ , and the second  $\pm$  corresponds to the spin directions  $\uparrow (\downarrow)$ , respectively. At half filling, no ferromagnetic moments exist because the lower two bands with opposite spin configurations are both fully occupied. However, at finite doping  $\delta$ , they are occupied differently, thus a spin polarization appears along the  $[110]$  direction. At very small doping, the ferromagnetic moment per site can be estimated from the dispersion relation of Eq. (3) as

$$\frac{M}{\delta} = \begin{cases} |\lambda/\chi| & \text{at } |\lambda/\chi| \ll 1 \\ |\chi/\lambda| & \text{at } |\chi/\lambda| \ll 1 \end{cases}. \quad (4)$$

It is instructive to consider the underlying symmetry reasons for this effect: the DDW order breaks the time reversal (TR) symmetry in the orbital channel while ferromagnetism breaks it in the spin channel. SO coupling couples two channels together to linear order. We emphasize that the polarization along the  $[110]$  direction is valid for *general* values of  $\lambda_{1,2}$ . This is protected by the following symmetry structures. Although the symmetries (i) and (iii) are broken by the DDW order, their combination with the TR operation together still leave the system invariant. These symmetries fix the only possible spin polarization along the  $[110]$  direction, and further exclude the antiferromagnetic order.

Now we consider the general values of  $\lambda_{1,2}$  with the parameterization  $\lambda_1 = \lambda \cos\theta$ ,  $\lambda_2 = \lambda \sin\theta$  ( $\theta = 0^\circ - 90^\circ$ ). The realistic values in  $\text{La}_{2-x}\text{Ba}_x\text{CuO}_4$ , i.e.,  $\lambda_1 \ll \lambda_2$ , correspond to  $\theta = 90^\circ$ . The new effective Hamiltonian includes Eq. (2) but with the replacement of  $\lambda$  with  $\lambda(\cos\theta + \sin\theta)/\sqrt{2}$ , and also an extra term of

$$\Delta H = -2i \sum_{\vec{k}, \alpha\beta} \{ \Delta \lambda g(k) c_{k\alpha}^\dagger \sigma_{2,\alpha\beta} c_{\vec{k}+\vec{Q},\beta} - \text{H.c.} \}, \quad (5)$$

where  $g(k) = \cos k_x + \cos k_y$ ,  $\sigma_2 = (\sigma_x - \sigma_y)/\sqrt{2}$ , and  $\Delta \lambda = \lambda(\sin\theta - \cos\theta)/\sqrt{2}$ . Correspondingly, the spin quantization axis of the electron eigenstate depends on the momentum  $\vec{k}$ , which deviates from the  $[110]$  direction with an angle  $\phi_k$  satisfying  $\tan\phi_k = \frac{k_{\perp}}{k_{\parallel}} \frac{\sin\theta - \cos\theta}{\sin\theta + \cos\theta}$ . This helical structure reduces the magnitude of the ferromagnetic moments. However, due to the fact that  $t_{\text{eff}}$  is much larger than  $\chi$  and  $\lambda$ , the Dirac cone is highly anisotropic. Then  $k_{\parallel} \gg k_{\perp}$  holds on most part of the Fermi pocket, and the spin deviates from the  $[110]$  direction only at small angles. In other words, the induced ferromagnetic moment is insensitive to the ratio of  $\lambda_1/\lambda_2$ .

In Fig. 2, we show the numerical results for the spin polarization per site  $M$  with the general values of  $\theta$  at  $\delta = 0.1$  and  $T = 0$  K by using the standard self-consistent method [21]. We choose parameters  $\lambda = 0.02$ ,  $V = 0.22$  to agree with the physical value of SO coupling and to arrive at a reasonable pseudogap energy scale in  $\text{La}_{2-x}\text{Ba}_x\text{CuO}_4$ . In the realistic case of  $\theta = 90^\circ$ , the polarization only decreases about 15% compared with its

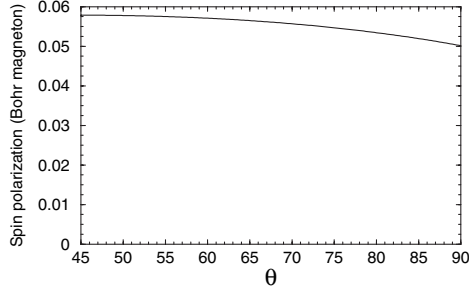


FIG. 2. Spin polarization in the LTO phase at doping  $\delta = 0.1$  with  $\lambda_1 = \lambda \cos\theta$ ,  $\lambda_2 = \lambda \sin\theta$  ( $45^\circ \leq \theta \leq 90^\circ$ ). The results within the range  $0^\circ \leq \theta \leq 45^\circ$  are symmetric to the case of  $90^\circ - \theta$ .

maximal value at  $\theta = 0^\circ$ . For all numeric results below, we keep  $\theta = 90^\circ$ , i.e.,  $\lambda_1 = 0$ . We further show  $M$  and  $\text{Im}\chi$  versus the doping  $\delta$  at  $T = 0$  K in Figs. 3(a) and 3(b). At low doping  $\delta$ ,  $M$  indeed scales with  $\delta$  linearly as indicated in Eq. (4). As  $\delta$  increases,  $\text{Im}\chi$  drops, and consequently  $M$  increases faster than linearly.

The finite temperature behavior of the induced polarization  $M$  is also interesting as shown in Fig. 4. At small dopings (e.g.,  $\delta = 0.06$ ),  $M$  increases slowly at low  $T$  and decreases after  $T$  passes an intermediate value, while  $M$  decreases monotonically at high dopings (e.g.,  $\delta = 0.12$ ). At low dopings,  $\text{Im}\chi$  is large at  $T = 0$  K which decreases with increasing  $T$ . As a result, the ratio  $\lambda/\text{Im}\chi$  increases, and so does  $M$  as indicated in Eq. (4). As  $T$  goes large, then the thermal effect dominates and  $M$  decreases. At high

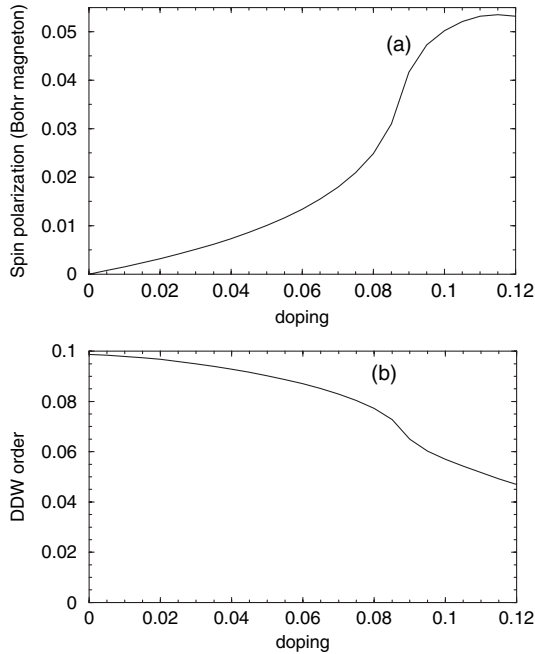


FIG. 3. (a) Spin polarizations  $M$  vs doping levels  $\delta$  at  $T = 0$  K. (b) The DDW order parameter  $\text{Im}\chi$  vs doping levels  $\delta$  at  $T = 0$  K.

dopings where  $\text{Im}\chi$  is comparable to  $\lambda$ ,  $M$  depends less sensitively on  $\lambda/\text{Im}\chi$ , and thus thermal effects dominate in the whole temperature range.

The magnitude of the induced moments is at the order of  $10^{-2}\mu_B$  which should be detectable. Because of their ferromagnetic nature, domain wall structures should be formed and no macroscopic magnetic field is present. A hysteresis behavior appears when an external in-plane magnetic field is applied to the sample. In the neutron scattering experiment, the elastic Bragg peaks at reciprocal lattice vectors are the evidence for these moments. The muon spin relaxation is also sensitive to the internal magnetic fields. To our knowledge, no such effects have been detected in the LTO phase of  $\text{La}_{2-x}\text{Ba}_x\text{CuO}_4$ .

SO coupling also leads to a “staggered spin galvanic effect” as the inverse of the DDW induced ferromagnetism. Assuming that the DDW order does not exist in the ground state, or equivalently setting  $V = 0$  in Eq. (1), and adding the Zeeman energy term  $H_z = -\sum_i g\mu_B \vec{B} \cdot \vec{S}_i$ , we find that a spin polarization along the  $[110]$  direction induces a staggered orbital current. The staggered current per bond is written as

$$I_{\text{stag}} = \frac{ie t_{\text{eff}}}{N\hbar} \sum_{k\sigma} c_{k\sigma}^\dagger c_{k+Q\sigma} f(\vec{k}) + \frac{e}{\sqrt{2}N\hbar} \sum_{k,\alpha\beta} c_{k\alpha}^\dagger c_{k\beta} \{(\lambda_1 \cos k_x + \lambda_2 \cos k_y) \sigma_{x,\alpha\beta} + (\lambda_2 \cos k_x + \lambda_1 \cos k_y) \sigma_{y,\alpha\beta}\}, \quad (6)$$

where the second term originates from SO coupling. Under the symmetry analysis,  $I_{\text{stag}}$  can be induced only by the  $B$  field along the  $[110]$  direction. Using the values of  $t_{\text{eff}}$  and  $\lambda$  stated above, the lattice constant  $a = 3.8 \text{ \AA}$ , and  $\theta = 90^\circ$ , we show in Fig. 5 the linear behavior of the staggered orbital moment per plaquette versus Zeeman energy  $E_z = \frac{1}{2} g\mu_B B$ . The magnitude reaches the order of  $10^{-3}\mu_B$  at  $E_z \approx 1 \text{ meV}$  which corresponds to  $B \approx 10 \text{ T}$ . The typical value of the DDW orbital moment estimated theoretically is at the order of  $10^{-2}\mu_B$  [9]. Compared with it, our induced orbital moment is about one order smaller.

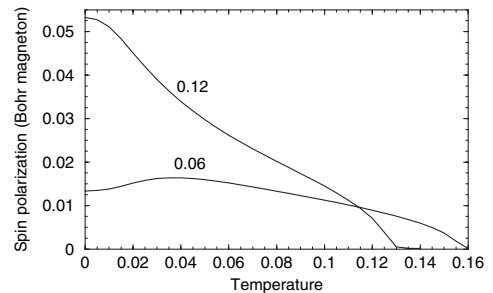


FIG. 4. Spin polarization vs temperatures at  $\delta = 0.06, 0.12$ . Temperatures are in the unit of  $t_{\text{eff}}$ .

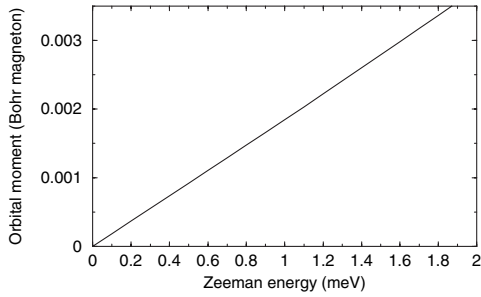


FIG. 5. Staggered orbital moment in the unit of  $\mu_B$  vs the Zeeman energy  $E_z = g/2B\mu_B$ , where  $t_{\text{eff}} = 100$  meV,  $\lambda/t_{\text{eff}} = 0.02$ ,  $\Delta\lambda = 0$ , and the Lande factor  $g = 2$ .  $\vec{B}$  is along the [110] direction.

In the LTT phase, the lattice symmetry results in a different staggered SO coupling pattern as  $\vec{\lambda}_{i,i+\hat{x}} = (-)^{i_x+i_y}(\lambda_1, 0, 0)$ ,  $\vec{\lambda}_{i,i+\hat{y}} = -(-)^{i_x+i_y}(\lambda_2, 0, 0)$  [19], where the spin quantization is fixed along the [100] direction and also  $\lambda_1 \ll \lambda_2$  [20]. Similar analysis indicates that the previous results also apply here with the replacement of the [110] with the [100] direction.

Next we discuss the effect of SO coupling in the superconducting portion of the phase diagram. SO coupling does not change the nature of the DSC phase in the absence of the DDW order. Because of the conservation of the TR symmetry, no ferromagnetic moment can appear. Although the spin and the fourfold rotational symmetries are broken, symmetries (ii) and (iii) still leave the  $d$ -wave singlet pairing structure unchanged, and thus the node quasiparticles are kept. In the coexisting region of DDW and DSC, if the DDW order is large compared with the DSC, the induced ferromagnetism suppresses the superconductivity, which may lead to Fulde-Ferrell-Larkin-Ovchinnikov phases [22].

At last, we briefly discuss the  $\text{YBa}_2\text{Cu}_3\text{O}_{6+\delta}$  system. The inversion symmetry is broken in each CuO plane, and the resulting SO coupling is uniform in contrast to the staggered pattern in  $\text{La}_{2-x}\text{Ba}_x\text{CuO}_4$  systems. Because of the existence of CuO chains, the [100] and [010] directions are not equivalent anymore, and the fourfold rotational symmetry is broken, while the reflection symmetries with respect to [100] and [010] directions are still kept. A straightforward symmetry analysis gives the form of the SO coupling [17] as  $\vec{\lambda}_{i,i+\hat{x}} = (0, \lambda_1, 0)$ ,  $\vec{\lambda}_{i,i+\hat{y}} = (\lambda_2, 0, 0)$ . However, because the staggered orbital current still preserves the above two reflection symmetries, this SO coupling cannot induce magnetic moments on Cu sites. We notice that at least in a single plane the broken parity has a significant effect in the superconducting phase: as in the 2D Rashba system the singlet and triplet pairing channels should be mixed [23].

In summary, we have investigated the effect of SO coupling to the DDW state in doped  $\text{La}_{2-x}\text{Ca}_x\text{CuO}_4$ . If the DDW state indeed exists, SO coupling results in a uniform ferromagnetic moment along the [110] direction in the LTO phase or the [100] direction in the LTT phase. This effect can be used to test the validity of the DDW scenario for the pseudogap mechanism. The inverse effect is also predicted that an in-plane Zeeman field induces a staggered orbit moment.

We thank S. Chakravarty and O. Vafek for helpful discussions. This work is supported by the NSF under Grant No. DMR-0342832, and U.S. Department of Energy, Office of Basic Energy Sciences under Contract No. DE-AC03-76SF00515. C.W. is supported by the Stanford Graduate program, and the NSF Grant No. Phy99-07949. J.Z. acknowledges financial support by the Fulbright foundation.

\*On leave of absence from the Instituut-Lorentz for Theoretical Physics, Leiden University, Leiden, The Netherlands.

- [1] S. Chakravarty *et al.*, Phys. Rev. B **63**, 094503 (2001).
- [2] C. Nayak, Phys. Rev. B **62**, 4880 (2000).
- [3] I. Affleck *et al.*, Phys. Rev. B **38**, 745 (1988).
- [4] J. O. Fjærestad *et al.*, Phys. Rev. B **65**, 125106 (2002).
- [5] C. Wu *et al.*, Phys. Rev. B **68**, 115104 (2003).
- [6] M. Tsuchiizu *et al.*, Phys. Rev. B **66**, 245106 (2002).
- [7] U. Schollwock *et al.*, Phys. Rev. Lett. **90**, 186401 (2003).
- [8] S. Capponi *et al.*, Phys. Rev. B **70**, 220505(R) (2004).
- [9] S. Chakravarty *et al.*, Int. J. Mod. Phys. B **15**, 2901 (2001).
- [10] H. A. Mook *et al.*, Phys. Rev. B **66**, 144513 (2002).
- [11] H. A. Mook *et al.*, Phys. Rev. B **69**, 134509 (2004).
- [12] C. Stock *et al.*, Phys. Rev. B **66**, 024505 (2002).
- [13] S. Murakami *et al.*, Science **301**, 1348 (2003).
- [14] J. Sinova *et al.*, Phys. Rev. Lett. **92**, 126603 (2004).
- [15] Y. K. Kato *et al.*, Science **306**, 1910 (2004); J. Wunderlich *et al.*, Phys. Rev. Lett. **94**, 047204 (2005).
- [16] I. Dzyaloshinskii, J. Phys. Chem. Solids **4**, 241 (1958); T. Moriya, Phys. Rev. **120**, 91 (1960).
- [17] T. Thio *et al.*, Phys. Rev. B **38**, R905 (1988).
- [18] D. Coffey *et al.*, Phys. Rev. B **44**, 10 112 (1991); D. Coffey *et al.*, Phys. Rev. B **42**, 6509 (1990).
- [19] N. E. Bonesteel *et al.*, Phys. Rev. Lett. **68**, 2684 (1992).
- [20] L. Shekhtman *et al.*, Phys. Rev. Lett. **69**, 836 (1992); D. Coffey *et al.*, Phys. Rev. B **46**, 5884 (1992); L. Shekhtman *et al.*, Phys. Rev. B **47**, 174 (1993); W. Koshibae *et al.*, Phys. Rev. B **50**, 3767 (1994); K. V. Tabunshchik *et al.*, Phys. Rev. B **71**, 214418 (2005); M. Silva Neto *et al.*, cond-mat/0502588; N. E. Bonesteel, Phys. Rev. B **47**, 11 302 (1993).
- [21] C. Wu *et al.*, Phys. Rev. B **66**, 020511(R) (2002); J. Zhu *et al.*, Phys. Rev. B **57**, 13 410 (1998).
- [22] P. Fulde *et al.*, Phys. Rev. **135**, A550 (1964); A. I. Larkin *et al.*, Sov. Phys. JETP **20**, 762 (1965).
- [23] L. P. Gor'kov *et al.*, Phys. Rev. Lett. **87**, 037004 (2001).